



Spatial changes in soil stable isotopic composition in response to carrion decomposition

Sarah W. Keenan^{1,2}, Sean M. Schaeffer¹, and Jennifer M. DeBruyn¹

¹University of Tennessee, Department of Biosystems Engineering and Soil Science, 2506 E.J. Chapman Drive, Knoxville, TN 37996

²Current address: South Dakota School of Mines and Technology, Department of Geology and Geological Engineering, 501 E. St. Joseph Street, Rapid City, SD 57701

Corresponding authors: sarah.keenan@sdsmt.edu, jdebruyn@utk.edu



Abstract

Decomposition provides a critical mechanism for returning nutrients to the surrounding environment. In terrestrial systems, animal carcass, or carrion, decomposition results in a cascade of biogeochemical changes. Soil microbial communities are stimulated, resulting in

5 transformations of carbon (C) and nitrogen (N) sourced from the decaying carrion soft tissues, changes to soil pH and electrical conductivity as microbial communities release CO₂ and mineralize organic N, and significant changes to oxygen availability. Over time, microbial communities transform ammonium to nitrate and potentially N₂O through nitrification and denitrification. While many of the rapid changes to soil biogeochemistry observed during carrion

10 decomposition return to background or starting conditions shortly after soft tissues are degraded, some biogeochemical parameters, particularly bulk soil stable $\delta^{15}\text{N}$ isotopic composition, have the potential to exhibit prolonged perturbations, extending for several years. The goal of this study was to evaluate the lateral and vertical changes to soil stable isotopic composition one year after carrion decomposition in a forest ecosystem. Lateral transects extending 140 cm from three

15 decomposition “hotspots” were sampled at 20 cm intervals, and subsurface cores were collected beneath each hotspot to a depth of 50 cm. Bulk soil stable isotopic composition ($\delta^{15}\text{N}$ and $\delta^{13}\text{C}$) indicated that one year after complete soft tissue removal and decay, soils were significantly ¹⁵N-enriched compared to control soils up to 60 cm from the hotspot center, and enrichment extended to a depth of 10 cm. Our results demonstrate that carrion decomposition has the potential to

20 result in long-term changes to soil biogeochemistry, up to at least one year after soft tissue degradation, and to contribute to bulk soil stable isotopic composition.



1 Introduction

25 Nutrient hotspots are introductions of carbon (C) and nitrogen (N)-rich compounds into
an ecosystem, resulting in elevated reaction rates compared to surrounding regions (McClain et
al., 2003). For terrestrial and aquatic systems, hotspots may be sourced from fallen trees (Lodge
et al., 2016), annual deposition of deciduous leaves (Vidon et al., 2010), animal scat (Erskine et
al., 1998; van der Waal et al., 2011), or animal carcasses (Parmenter and Lamarra, 1991; Carter
30 et al., 2007; Wheeler et al., 2014; Wheeler and Kavanagh, 2017). Hotspots sourced from animal
carcasses, also referred to as carrion hotspots, significantly alter surface and belowground soil
physiochemistry and plant communities in terrestrial ecosystems (Carter et al., 2007; Keenan et
al., 2018). These alterations can have significant long-term impacts; for example large animal
carcasses had measurable effects on a prairie ecosystem for at least 5 years (Towne, 2000), and a
35 decade or more in the Arctic (Danell et al., 2002). In addition to providing a critical source of C
and N, carrion hotspots are important sources of ecosystem heterogeneity (Towne, 2000; Bump
et al., 2009b) and promote biodiversity (Barton et al., 2013).

Carrion decomposition occurs in a series of physical (Payne, 1965) and biogeochemical
(Keenan et al., 2018) stages. The breakdown and release of animal tissues provides a labile
40 source of nutrients for insect and animal scavengers as well as soil microfauna (i.e., bacteria,
fungi, nematodes). Studies evaluating the consequences of carrion decay on soil biogeochemistry
have monitored decomposition on a range of timescales, from days (Metcalf et al., 2013;
Macdonald et al., 2014; Keenan et al., 2018; Szelecz et al., 2018) to years (Towne, 2000; Bump
et al., 2009a; Keenan et al., *in press*), and in different climatic and geographic settings, including
45 temperate forests (Melis et al., 2007; Cobaugh et al., 2015; Keenan et al., 2018) and Australian
rangeland (Macdonald et al., 2014), as well as under controlled laboratory settings (Carter et al.,



2008, 2010). Some of the key changes that occur in soils following the deposition and decomposition of carrion include: changes to pH, electrical conductivity, oxygen availability, gas fluxes (CO_2 , CH_4 , N_2O , H_2S), elevated rates of microbially-driven C and N cycling, and
50 dissolved compounds available to microbes (NH_4^+ , NO_3^- , Ca^{2+} , SO_4^{2-}) (Melis et al., 2007; Aitkenhead-Peterson et al., 2012; Keenan et al., 2018).

Many of the rapid, pulsed perturbations to soil C and N pools observed at carrion hotspots, such as elevated microbial respiration rates (measured as CO_2 release) and changes to soil pH, return to background biogeochemical conditions during the skeletal stage of
55 decomposition, when soft tissues have been largely or completely degraded by insect and animal scavengers (Cobaugh et al., 2015; Keenan et al., 2018). However, certain biogeochemical measures, including soil stable $\delta^{15}\text{N}$ composition, have been observed to remain enriched in soils collected at carrion hotspots compared to background soils for a protracted period of time, up to several years (Bump et al., 2009a ; Wheeler and Kavanagh, 2017). Soil stable isotopic
60 composition integrates all biogeochemical activity within the soil as well as inputs from plant or animal matter. In contrast with $\delta^{15}\text{N}$ enrichment, no changes in soil $\delta^{13}\text{C}$ composition have been observed in surface soils of decomposition hotspots (Wheeler and Kavanagh, 2017; Keenan et al., 2018). A variety of studies have demonstrated the potential for natural abundances of ^{15}N to be used as a tracer of ecological processes, including N input from animals (urea and feces) in N-
65 limited and isolated ecosystems (Erskine et al., 1998) and input of marine taxa (salmon carcasses) to terrestrial and riparian areas (Kline et al., 1990; Koyama et al., 2005).

While ^{15}N enrichment due to carrion decomposition has been demonstrated in previous work, these studies were limited to surface soils (maximum sampling depth of 10 cm) from the center of the hotspots (Bump et al., 2009a; Wheeler and Kavanagh, 2017). This has left a gap in



70 our understanding of the spatial extent of carcass enrichment, which is ultimately necessary for
quantifying ecosystem impacts of these decomposition inputs. Given the potential for natural
abundance ^{15}N to serve as a long-term tracer of decomposition processes, the goal of this study
was to evaluate spatial changes in stable ^{15}N -enrichment at a carrion hotspot one year post-
decay. In particular, the lateral and vertical extent of stable isotope changes as a result of
75 enhanced biogeochemical reactions in a hotspot is largely unknown. Soils beneath and adjacent
to former carrion hotspots (up to ~40 cm, the extent of visible fluid migration) were expected to
remain ^{15}N -enriched one year after decay. Additionally, isotopic enrichment was expected to
persist to at least 10 cm depth, the maximum depth examined in previous studies.

80 **2 Materials and Methods**

2.1 Study area and sample collection

The study site was a mixed deciduous forest in East Tennessee (36°0'1.0" N, 84°13'1.6"
W, ~330 m elevation). Soils were part of the Fullerton-Pailo complex and characterized as Typic
Paleudults (Soil Survey Staff, 2018). The A horizon extended to approximately 20 cm depth.
85 Five ~23 kg nuisance North American beaver (*Castor canadensis*) carcasses were placed frozen
within scavenger prevention enclosures (1.19 x 0.74 x 0.81 m) and allowed to decay naturally,
starting 31 July 2016. As part of a separate study, approximately 75 g of surface soil (0-5 cm
depth) was collected a total of five times during decay beneath each animal (Keenan et al.,
2018). For this study, soils were collected on 8 August 2017, one year after decomposition, and
90 after bones had been removed from the site. Soils were taken from surface transects as well as
from cores obtained at depth below three carrion hotspots. Approximately 30 g of soil from the
top 0-5 cm were collected using a 3 cm diameter auger within the hotspot—an area 80 cm in



diameter of visibly discolored soil. Surface samples were additionally collected along a linear transect radiating from the hotspot at 20 cm intervals up to 140 cm (Fig. 1). Within the hotspots, 95 soils were cored to a depth of 50 cm using a 10 cm diameter auger; cores were partitioned into depth intervals of 0-5, 5-10, 10-15, 15-20, 20-30, 30-40, and 40-50 cm depth (Fig. 1).

All soil samples were homogenized to a uniform consistency in the field by hand (changing nitrile gloves between samples), removing any rocks, roots, leaves, or vegetation larger than 2 mm. Samples were transported to the lab and processed immediately. Aliquots were 100 oven-dried in triplicate at 105°C for 48 h to determine gravimetric moisture (Table 1, Table S1). Once dried, subsamples were powdered in an agate mortar and pestle and stored in 1.5 mL tubes until subsequent isotopic analyses. Samples (~25 mg) were transferred into 5 × 9 mm tin capsules (Costech). Isotopic analyses were conducted at Washington University in St. Louis. Samples, standards, and blanks were loaded into a Costech Zero Blank autosampler and 105 combusted in a Flash 2000 elemental analyzer. Soil $\delta^{13}\text{C}$ and $\delta^{15}\text{N}$ values were measured on a Delta V Plus continuous-flow (ConFlo IV, Thermo Fisher Scientific), isotope-ratio-mass spectrometer. Standards included millet and acetanilide. Millet was used to evaluate linearity. Sample carbon isotopic values were corrected for sample size and instrument drift using millet and acetanilide, and nitrogen values were corrected using millet, acetanilide, and urea. Analytic 110 precision was <0.2 ‰ for both carbon and nitrogen. Results are presented in δ notation as parts per mil (‰) where $\delta^{13}\text{C} = [((^{13}\text{C}/^{12}\text{C}_{\text{sample}} / ^{13}\text{C}/^{12}\text{C}_{\text{standard}}) - 1) \times 1,000]$ and $\delta^{15}\text{N} = [((^{15}\text{N}/^{14}\text{N}_{\text{sample}} / ^{15}\text{N}/^{14}\text{N}_{\text{standard}}) - 1) \times 1,000]$. Vienna Pee Dee Belemnite was used as the carbon standard and air was used for nitrogen.

Soils collected from the center (0-5 cm depth) of all five hotspots and a composite control 115 sample (pooled soil collected from five locations ~3 m from each hotspot) were also analyzed for



microbial respiration rates (as evolved CO₂), ammonium, nitrate, nitrification potential, pH, electrical conductivity, dissolved organic C and N, and protein content, building from a previous study at the site and following the methods described by Keenan et al. (2018). In brief, headspace CO₂ was measured immediately after placing and sealing soil into 60 mL serum vials, as well as after 24 h (LI-820, Licor Inc.). Vacuum-filtered (1 µm; Ahlstrom, glass microfiber) soil extracts (10 g soil: 40 mL 0.5 M K₂SO₄) were collected after shaking for 4 hours at 150 rpm at room temperature, and were frozen at -20°C until subsequent colorimetric analysis of ammonium and nitrate (Rhine et al., 1998; Doane and Horwath, 2003). Aliquots were oxidized with a persulfate solution to measure dissolved organic carbon (DOC) as evolved CO₂ and dissolved organic nitrogen (DON) colorimetrically as nitrate (Doyle et al., 2004). Nitrification potential was determined colorimetrically using a modified chlorate block method optimized for microplates (Belser and Mays, 1980; Keeney and Nelson, 1982; Hart, 1994). Soil pH and electrical conductivity were measured from a soil slurry (3 g soil: 6 mL deionized water) using a handheld multi-parameter meter (Orion A329, Thermo Scientific). Protein content was determined using the Bradford Assay (Wright and Upadhyaya, 1996; Redmile-Gordon et al., 2013). Because the goal of this study was to focus specifically on stable isotopes as long-term tracers in carrion hotspots, only surface soils from the five remnant hotspot centers were processed for full physiochemistry.

2.2 Stable isotope analyses

The contribution of carcass-derived nitrogen to bulk soil stable isotopic composition in surface transects was determined using a linear two-member isotope mixing model (Wheeler and Kavanagh, 2017; Keenan et al., 2018), using bulk control soil δ¹⁵N composition (0.1 ‰) as one



end-member and beaver decomposition fluid (10.2 ‰) as the other. Decomposition fluid is the
140 by-product of microbial and autolytic processes acting on a carcass after animal death. Fluids
consist of amino acids, dead and live microbial cells, urea, water, and lipids, and represent one of
the primary mechanisms for return of host's tissues to the surrounding environment.
Decomposition fluid isotopic composition was previously determined, using fluids collected
from three decomposing beavers left on a shallow plastic tray to intercept fluids (Keenan et al.,
145 2018). The linear equation for the isotope mixing model (Wheeler and Kavanagh, 2017) was
defined as:

$$CDN = [(TEM - SEM)/(FEM - SEM)] \times 100$$

Where CDN is the carcass-derived N (%), TEM is the average $\delta^{15}\text{N}$ of soil from the treatment
condition (sampling interval along the surface transects), SEM is the end-member control soil
stable isotopic composition (0.1 ‰), and FEM is the end-member isotopic composition of
150 decomposition fluids (10.2 ‰). The contribution of control soil-derived $\delta^{15}\text{N}$ to measured
treatment conditions was calculated by subtracting CDN (%) from 100 %.

The contributions of multiple sources to bulk soil stable isotopic composition ($\delta^{13}\text{C}$ and
 $\delta^{15}\text{N}$) were assessed using Stable Isotope Analysis in R (SIAR) using the *simmr* package (Parnell
et al., 2010). Three sources were integrated into the modeling: (1) surface control soils, (2)
155 decomposition fluids, and (3) control soils at depth (40 cm). Soil $\delta^{13}\text{C}$ and $\delta^{15}\text{N}$ composition at
each depth were modeled to assess which source exerted a greater influence on bulk soil isotopic
composition.

To track changes in $\delta^{15}\text{N}$ between surface soil and soil collected at depth, $\Delta^{15}\text{N}$ values
were calculated by subtracting the $\delta^{15}\text{N}$ value of soil at each depth from values obtained at the



160 surface of the hotspot and control sampling locations. Negative $\Delta^{15}\text{N}$ values indicate that surface
soils are ^{15}N -enriched compared to soils at depth (Martinelli et al., 1999).

2.3 Statistical analyses

Data were analyzed using SigmaPlot to test for significant differences between treatments
165 and controls. For both surface and depth transects, data from the three transects were treated as
replicates for subsequent statistical analyses. Significance ($p < 0.05$) was determined based on
one-way ANOVA analyses with Holm-Sidak post-hoc testing. Significant differences between
control and hotspot soils were determined using paired t-tests at each sampling depth or transect
interval using R (R Core Team, version 3.5.0).

170

3 Results

3.1 Surface soil biogeochemical changes during decomposition

During carrion decomposition, fluids sourced from the carcass were released into the
surrounding environment (Fig. 2). The pulse of nutrient-rich fluids resulted in significant
175 changes to surrounding soil physiochemistry (Table 1, Table S1). Soils exhibited long-term
changes to physiochemistry following fluid degradation by soil microbial communities. In
particular, after one year of decay, soil pH was significantly lower than control, initial, and pre-
decay soils ($p < 0.001$; $F = 59.317$). In addition, bulk soil $\delta^{15}\text{N}$ remained significantly enriched
compared to control and starting soil isotopic composition ($p < 0.001$; $F = 27.948$). Other
180 physicochemical parameters, including conductivity, microbial respiration, DOC, DON,
ammonium, nitrate, and nitrification potential all returned to background conditions after one



year. With the exception of the one year samples, data were previously published in Keenan et al. (2018) and are included here for comparison.

185 3.2 Lateral changes in stable isotopic composition

Soils were significantly ^{15}N -enriched within the visible carrion hotspot (mean soil composition $7.5 \pm 1.0 \text{ ‰}$) and up to 60 cm from the hotspot center ($2.2 \pm 0.5 \text{ ‰}$) compared to composite control soils (0.1 ‰) (Fig. 3, Table S2) (paired t-test, $p = 0.016$). Soil $\delta^{15}\text{N}$ values gradually declined, reaching background abundance values around 80 cm of the hotspot center.

190 In contrast, there were no significant differences between control and hotspot soil $\delta^{13}\text{C}$, and no differences as a function of distance from the hotspot center (one-way ANOVA, $p = 0.464$; $F = 1.004$). C/N ratios were lower within the hotspot and exhibited a gradual and significant increase with increasing distance from the hotspot center (Fig. 3). However, there were no significant differences between hotspot and control soil C/N.

195 The influence of carrion decomposition on soil stable $\delta^{15}\text{N}$ isotopic composition decreases with increasing distance from the hotspot (Figs. 3a, S1). Soil C:N composition follows a linear trend, increasing by 0.07 per cm from the hotspot center (Fig. S1). Based on linear two-member isotope mixing models, carcass-derived fluids exhibit a linear decrease in contributions to soil isotopic composition with increasing distance from the hotspot. Carcasses contribute to
200 soil stable $\delta^{15}\text{N}$ isotopic composition up to 60 cm from the hotspot center (Fig. 4), an area that was not visibly discolored as observed within the center of the hotspot (Fig. 2).

3.3 Vertical changes in stable isotopic composition



Soil collected at depth beneath the three mortality hotspots was significantly ^{15}N -enriched
205 compared to control soils up to 10 cm depth (Fig. 5). Surface hotspot soils were also enriched at
30 cm depth compared to the control. Control soils became more ^{15}N -enriched with increasing
depth. There was no significant difference between control and hotspot soil $\delta^{13}\text{C}$ and C/N values,
and both exhibited the same trends with depth. Soils exhibited ^{13}C -enrichment with increasing
depth and a decline in C/N ratios.

210 Control soils exhibited a strong positive linear relationship between the negative of the
natural log of bulk soil %N and %N and stable isotopic composition, reflecting decreasing N and
C availability with increasing depth. Decomposition results in a shift in the hotspot soil N
isotopic discrimination factor (D , or the slope of the linear regressions) (Natelhoffer and Fry,
1988), leading to a less positive slope compared to control soils (Fig. 6). D does not change for C
215 isotopes in control or hotspot soils.

In general, soils exhibit a trend of increasing $\Delta^{15}\text{N}$ (the difference between soil $\delta^{15}\text{N}$
value at a specific depth and $\delta^{15}\text{N}$ at the surface) with depth, reflecting ^{15}N -enrichment in deep
forest soils (Martinelli et al., 1999). Hotspot soils exhibited lower $\Delta^{15}\text{N}$ values compared to
control soils, indicating little change in ^{15}N -enrichment with depth (Table 2). Control soils
220 displayed increasing $\Delta^{15}\text{N}$ with depth, a pattern globally observed in forest soils (Martinelli et al.,
1999) (Table 2). Combined with D (Fig. 6), hotspot and control vertical profiles have distinct N
sources and exhibit distinct isotopic enrichment patterns with depth.

Stable isotope mixing models evaluated the proportional contribution of three distinct
sources to soil stable isotopic composition in hotspot depth profiles: control surface soils,
225 decomposition fluids, and control soils at 40 cm depth. Because the lateral influence of
decomposition on soil $\delta^{15}\text{N}$ composition did not extend beyond 60 cm in surface soils, samples



collected at 100, 120, and 140 cm were included in the control surface soil average (-0.1 ± 0.3 ‰). Soils collected from 0-5 cm exhibited a significant contribution from decomposition fluids (Fig. 7a,b). As depth increases beyond 10 cm, there is no change to the proportional contribution
230 of decomposition fluid to bulk stable isotopic composition. By 30-40 and 40-50 cm depth, hotspot soil $\delta^{15}\text{N}$ and $\delta^{13}\text{C}$ compositions are similar to control soils (Fig. 7a), indicating limited, if any, input from decomposition fluids.

4 Discussion

235 Soils associated with carrion decomposition hotspots retained biogeochemical markers of vertebrate decay at least one year after soft tissue degradation. Within the hotspots, soils remained ^{15}N -enriched compared to control locations, suggesting that decomposing animals have the potential to exert long-term changes, here at least one year, on surface and subsurface soil stable isotopic composition. The beaver carcasses used this study, which were between 20 kg and
240 25 kg in mass, resulted in measurable changes down to 10 cm depth and out to 60 cm away from the center of the hotspot, beyond the area that was visibly discolored from decomposition fluids. The contribution of carcass-derived N to soils at depth as well as laterally is influenced by a variety of physical and climatic variables. Here, decay occurred during the summer in East Tennessee, with an average high of 32.2°C for the month of August. Carcasses were exposed to
245 measureable precipitation six out of 10 days after placement, preventing soft tissues from significant desiccation and supporting abundant blowfly larvae and other insect activity. Blowfly larvae migrating away from the carcasses on the surface and within the soil to pupate likely provided an important physical mechanism to distribute beaver-enriched N to surrounding soils. Blowfly larvae can potentially move up to 10 m away from the carcass, and typically extend



250 down into the soil up to 10 cm depth, depending on the soil substrate properties (Gomes et al.,
2006). As blowfly larvae disperse, they have the potential to physically transport decomposition
fluids acquired internally or externally during feeding, release excrement during migration, or
die, leaving their tissues to degrade. An estimated 65.9 % of pupae that disperse to pupate die en
route (Putman, 1977). Rainfall may have also contributed to the downward movement of
255 decomposition fluids.

The temporal persistence of isotopic enrichment hotspots is currently unknown, but is
likely to be ecosystem, carrion type, and carrion mass-specific. A larger carcass would be
expected to result in greater lateral and vertical dispersal of carrion-derived fluids, as well as
greater changes to ecosystem processes, because of the greater volume of decomposing soft
260 tissue (Baruzzi et al., 2018). In addition, larger carcasses may host a larger and longer-lived
insect community (Parmenter and MacMahon, 2009), including blowfly larvae, which may
further nutrient dispersal and may impact a larger area. Bump et al. (2009b) observed elevated
foliar $\delta^{15}\text{N}$ values in plants growing on sites impacted by deer carcass (~56 kg) decomposition at
least 2.5 years after decay in a temperate hardwood forest, suggesting a long-lived hotspot
265 signature. In some ecosystems, such as the Arctic tundra, isotopic enrichment is likely to persist
for even longer based on perturbations to C and N surrounding muskox after 5 to 10 years of
decay (Danell et al., 2002).

Increasing $\delta^{13}\text{C}$ and $\delta^{15}\text{N}$ values with depth in soils has previously been observed in a
variety of soil types and climatic conditions (Natelhoffer and Fry, 1988; Martinelli et al., 1999;
270 Billings and Richter, 2006). Changes to $\delta^{13}\text{C}$ with depth are due to progressive cycling of C
through microbial biomass (Liang et al., 2017), where selective preservation and biochemical
fractionation together lead to ^{13}C -enriched organic C in soil (Natelhoffer and Fry, 1988; Billings



and Richter, 2006). While we observed a similar increase in $\delta^{13}\text{C}$ with depth, we did not see a significant change in ^{13}C as a result of carcass enrichment. Wheeler and Kavanagh (2017) similarly did not observe a change in soil $\delta^{13}\text{C}$ following carrion decomposition.

Increasing $\delta^{15}\text{N}$ values with depth reflects two broad biochemical processes leading to fractionation, both likely driven by microbial activities. First, the preferential excretion of ^{15}N -depleted compounds during catabolism and anabolism leaves the residual microbial cells and soil ^{15}N -enriched. Second, kinetic fractionation associated with gaseous N loss is also known to result in enrichment, depending on the microbial communities present and N mineralization rates (Evans, 2001; Robinson, 2001; Liang et al., 2017). Over time, as soil profiles develop, accretion of ^{15}N -enriched microbial cells, particularly fungi, leads to isotopic enrichment at depth (Billings and Richter, 2006). In contrast, plant and leaf litter are the dominant contributors to N pools in surface soils in most temperate forest ecosystems (Vidon et al., 2010), resulting in surface soils that are isotopically-depleted compared to the soil profile at depth. Decomposition hotspots, however, disrupt the expected pattern (Fig. 5), causing surface enrichment, and likely leave a lasting impact on soil stable isotopic composition.

For systems at or near steady state conditions, the difference in isotopic enrichment between soils at depth and the surface ($\Delta^{15}\text{N}$) provides a way to compare soils from different geographic and climatic locations (Martinelli et al., 1999), and was used here to compare hotspot soils and those collected at control locations. $\Delta^{15}\text{N}$ values observed in the control depth profile are within the expected range observed in temperate forests worldwide (2.7 to 9.1 ‰) (Table 2). However, as a consequence of carrion inputs and decay, $\Delta^{15}\text{N}$ values are more similar to those observed in tropical forest ecosystems (1.1 to 4.3 ‰). In tropical systems, lower $\Delta^{15}\text{N}$ values are thought to reflect more open N cycling with elevated N losses (nitrification, nitrate leaching, and



ammonia volatilization) under conditions of elevated total N inputs (Martinelli et al., 1999).

Whether our observed changes in $\Delta^{15}\text{N}$ are due to elevated N cycling rates, disequilibrium effects across the soil profile due to changing N inputs from a system dominated by atmospheric dry and wet deposition of nitrate and ammonium to one with carrion-sourced N, or both, is not known.

300 The stable isotopic discrimination factors (D) did not differ for control and hotspot soil $\delta^{13}\text{C}$ (Fig. 6), suggesting that C cycling and pools in soils one year after carrion decay are not altered. In contrast, D values for $\delta^{15}\text{N}$ were different between control and hotspot soils. This indicates distinct N sources for the two soil profiles, emphasizing that decaying carrion provide an important and potentially distinct N pool for soil ecosystems. In addition, differences in D
305 values between the two soils suggest that there is less discrimination occurring within hotspot soils compared to control soils, likely due to the rapid input of an isotopically-enriched N pool (Evans, 2001).

Hotspot soils received the input of beaver-derived fluids ($10.2 \pm 0.4 \text{ ‰}$) (Keenan et al., 2018) as well as soft and hard tissues (1.0 to 4.0 ‰ for beaver bone collagen from Minnesota;
310 Fox-Dobbs et al., 2007). Stable isotope mixing models demonstrate that decomposition fluids are a significant contributing source to bulk soil stable isotopic composition up to 60 cm from the hotspot center (Fig. 4), and multi-source mixing models also suggest some contributions up to 10 cm depth (Fig. 7). Beyond 10 cm depth, there is a stable and uniform proportional contribution, with decomposition fluids not significantly influencing soil stable isotopic composition. Rather,
315 natural $\delta^{15}\text{N}$ enrichment due to soil accretion processes can explain the observed soil stable isotopic composition. Based on the isotopic discrimination factor (D) for N in hotspot soils, linear regression line for hotspots soil results in a predicted starting N source of 4.8 ‰, in line with the expected value for fresh beaver tissues (Fig. 6). This suggests that the stable isotopic



composition of soil $\delta^{15}\text{N}$, even one year after decay, may be a useful tool to infer starting animal
320 tissue isotopic composition.

5 Conclusions

Soil isotopic composition is controlled by the isotopic composition of input(s) and subsequent abiotic and biotic biogeochemical processes that potentially lead to fractionation. The
325 input of an isotopically-enriched source such as decomposing carrion resulted in significant spatial and temporal perturbations to soil stable isotopic composition. The decay of ~23 kg North American beavers resulted in rapid (within days) and long-lived (up to one year) ^{15}N -enrichment in forest soils up to 10 cm depth and ~60 cm distal. Soil biogeochemistry, particularly N cycling, is complex, and carrion inputs have the potential to alter expected patterns long after soft tissues
330 have been completely degraded.

Observed ^{15}N -enrichment at depth and laterally is likely due to a combination of physical movement of fluids during decomposition and the transport of fluids by insects, particularly blowfly larvae. In this system, rainfall during decomposition may have also acted as a physical transport mechanism. While likely to be significantly influenced by carcass size, climate, and
335 soil type, decomposition has the potential to exert long-lived influences on soil stable isotopic composition.

Data availability

All data generated in this study are available in the Supplement.



340 *Author contributions.* SWK and JMD designed the experiments. All authors assisted with data interpretation. JMD and SMS provided financial, lab, and analytical resources. SWK and JMD prepared the manuscript with contributions from SMS.

Competing interests. The authors declare that they have no conflict of interest.

345

Acknowledgements. Salvaged nuisance beavers were provided by the USDA, APHIS, Wildlife Services of East Tennessee. Lois S. Taylor, Jose Lique, Fei Yao, and Jialin Hu assisted with soil collection. Alex Bradley provided lab and instrument access, and Melanie Seuss assisted with stable isotopic analyses. This research was funded by a National Science Foundation Award

350 (EAG1549726) to JMD and SMS.

Figure and table legends

Figure. 1: Schematic cross-section view of the locations of soil samples (stars) collected from each of three carrion decomposition sites. Dashed line represents the hotspot—the area of visibly discolored soil. Soils collected at depth extended to the B horizon. The visibly discolored area of soil due to carrion hotspot formation extended approximately 35-40 cm from the hotspot center along the surface and to a few centimeters depth.

355

Figure 2: View of a beaver after placement (a) and during advanced decay (b) to demonstrate the lateral migration of carcass-derived fluids during decay. Both photos are from the same animal, and (b) were taken during advanced decay (8 August 2016). Visible extent of fluid migration is outlined in the white dashed line.

360



Figure 3: Lateral changes in soil stable (a) $\delta^{15}\text{N}$ and (b) $\delta^{13}\text{C}$ isotopic composition and (c) C/N
365 ratios extending from carrion hotspot centers. Soil was visibly discolored 35-40 cm from the
center (here, 0 cm distance). Letters indicate significant differences as a function of distance
based on an ANOVA and Holm-Sidak post-hoc test, and asterisks denote significant differences
between control and hotspot soils (t-test). The dashed line represents control surface soil (0-5
cm) composition.

370

Figure 4: Results of linear two-member isotope mixing distinguishing the contributions of soil
and carcass fluid to bulk soil stable isotopic composition.

Figure 5: Stable isotopic composition and C/N ratios for soils beneath carrion hotspots (closed
375 circles) and at a control location (stars). Letters indicate significant differences as a function of
depth, and asterisks indicate significant differences between control and hotspot soils (both based
on one-way ANOVA, $p < 0.05$).

Figure 6: Bulk soil stable isotopic composition and corresponding negative natural log %N (a)
380 and %C (b) for hotspot and control soils with depth. Linear regressions were fit to hotspot and
control datasets.

Figure 7: Stable isotope mixing models for hotspot soils collected at depth. (a) The three
potential sources contributing to soil $\delta^{13}\text{C}$ and $\delta^{15}\text{N}$ isotopic composition were used as inputs,



385 and exert different contributions at each depth. (b) The proportional contribution of
decomposition fluids changes as a function of depth.

References

- Aitkenhead-Peterson, J. A., Owings, C. G., Alexander, M. B., Larison, N., and Bytheway, J. A.:
390 Mapping the lateral extent of human cadaver decomposition with soil chemistry, *Forensic Sci.*
Int., 216, 127-134, <https://doi.org/10.1016/j.forsciint.2011.09.007>, 2012.
- Barton, P. S., Cunningham, S. A., Lindenmayer, D. B., and Manning, A. D.: The role of carrion
in maintaining biodiversity and ecological processes in terrestrial ecosystems, *Oecologia*, 171,
761-772, <https://doi.org/10.1007/s00442-012-2460-3>, 2013.
- 395 Baruzzi, C., Mason, D., and Lashley, M. A.: Effects of increasing carrion biomass on food webs,
Food Webs, 16, <https://doi.org/10.1016/j.fooweb/2018.e00096>, 2018.
- Belser, L. W., and Mays, E. L.: Specific inhibition of nitrite oxidation by chlorate and its use in
assessing nitrification in soils and sediments, *Appl. Environ. Microbiol.*, 39, 505-510, 1980.
- Billings, S. A., and Richter, D. D.: Changes in stable isotopic signatures of soil nitrogen and
400 carbon during 40 years of forest development, *Oecologia*, 148, 325-333,
<https://doi.org/10.1007/s00442-006-0366-7>, 2006.
- Bump, J. K., Peterson, R. O., and Vucetich, J. A.: Wolves modulate soil nutrient heterogeneity
and foliar nitrogen by configuring the distribution of ungulate carcasses, *Ecology*, 90, 3159-
3167, <https://doi.org/10.1890/09-0292.1>, 2009a.
- 405 Bump, J. K., Webster, C. R., Vucetich, J. A., Peterson, R. O., Shields, J. M., and Powers, M. D.:
Ungulate carcasses perforate ecological filters and create biogeochemical hotspots in forest



- herbaceous layers allowing trees a competitive advantage, *Ecosystems*, 12, 996-1007,
<https://doi.org/10.1007/s10021-009-9274-0>, 2009b.
- 410 Carter, D. O., Yellowlees, D., and Tibbett, M.: Cadaver decomposition in terrestrial ecosystems,
Naturwissenschaften, 94, 12-24, <https://doi.org/10.1007/s00114-006-0159-1>, 2007.
- Carter, D. O., Yellowlees, D., and Tibbett, M.: Temperature affects microbial decomposition of
cadavers (*Rattus rattus*) in contrasting soils, *Appl. Soil. Ecol.*, 40, 129-137,
<https://doi.org/10.1016/j.apsoil.2008.03.010>, 2008.
- Carter, D. O., Yellowlees, D., and Tibbett, M.: Moisture can be the dominant environmental
415 parameter governing cadaver decomposition in soil, *Forensic Sci. Int.*, 200, 60-66,
<https://doi.org/10.1016/j.forsciint.2010.03.031>, 2010.
- Cobaugh, K. L., Schaeffer, S. M., and DeBruyn, J. M.: Functional and structural succession of
soil microbial communities below decomposing human cadavers, *PLoS One*,
<https://doi.org/10.1371/journal.pone.0130201>, 2015.
- 420 Danell, K., Berteaux, D., and Brathen, K. A.: Effect of muskox carcasses on nitrogen
concentration in tundra vegetation, *Arctic*, 55, 389-392, 2002.
- Doane, T. A., and Horwath, W. R.: Spectrophotometric determination of nitrate with a single
reagent, *Anal. Lett.*, 36, 2713-2722, <https://doi.org/10.1081/AL-120024647>, 2003.
- Doyle, A., Weintraub, M. N., and Schimel, J. P.: Persulfate digestion and simultaneous
425 colorimetric analysis of carbon and nitrogen in soil extracts, *Soil Sci. Soc. Am. J.*, 68, 669-
676, 2004.
- Erskine, P. D., Bergstrom, D. M., Schmidt, S., Stewart, G. R., Tweedie, C. E., and Shaw, J. D.:
Subantarctic Macquarie Island—a model ecosystem for studying animal-derived nitrogen



- sources using ^{15}N natural abundance, *Oecologia*, 117, 187-193,
430 <https://doi.org/10.1007/S004420050647>, 1998.
- Evans, R. D.: Physiological mechanisms influencing plant nitrogen isotope composition, *Trends Plant Sci.*, 6, 121-126, [https://doi.org/10.1016/S1360-1385\(01\)01889-1](https://doi.org/10.1016/S1360-1385(01)01889-1), 2001.
- Fox-Dobbs, K., Bump, J. K., Peterson, R. O., Fox, D. L., and Koch, P. L.: Carnivore-specific stable isotope variables and variation in the foraging ecology of modern and ancient wolf
435 populations: case studies from Isle Royale, Minnesota, and La Brea, *Can. J. Zool.*, 85, 458-471, <https://doi.org/10.1139/Z07-018>, 2007.
- Gomes, L., Godoy, W. A. C., and Von Zuben, C. J.: A review of postfeeding larval dispersal in blowflies: implications for forensic entomology, *Naturwissenschaften*, 93, 207-215, <https://doi.org/10.1007/s00114-006-0082-5>, 2006.
- 440 Hart, S. C., Stark, J.M., Davidson, E.A., Firestone, M.K.: Nitrogen mineralization, immobilization, and nitrification, in: *Methods of soil analysis part 2: microbiological and biochemical properties*, Edited by: Weaver, R. W., Angle, S., Bottomley, P., Bezdicek, D., Smith, S., Tabatabai, A., Wollum, A., Soil Science Society of America, Madison, Wisconsin, 985-1018, 1994.
- 445 Keenan, S. W., Schaeffer, S. M., Jin, V. L., and DeBruyn, J. M.: Mortality hotspots: nitrogen cycling in forest soils during vertebrate decomposition, *Soil Biol. Biochem.*, 121, 165-176, <https://doi.org/10.1016/j.soilbio.2018.03.005>, 2018.
- Keenan, S. W., Emmons, A. L., Taylor, L. S., Phillips, G., Mason, A. R., Mundorff, A., Bernard, E.C., Davoren, J., and DeBruyn, J. M.: Soil physiochemistry and microbial ecology of a
450 multi-individual grave. *PLoS One*, <https://doi.org/10.1371/journal.pone.0208845>, *in press*.



- Keeney, D. R., and Nelson, M. H.: Nitrogen—inorganic forms, in: *Methods of soil analysis, part 2, chemical and microbiological methods*, Edited by: Page, A. L., Miller, D. R., and Keeney, D. R., American Society of Agronomy and the Soil Science Society of America, Madison, WI, 643-698, 1982.
- 455 Kline, T. C., Goering, J. J., Mathisen, O. A., Poe, P. H., and Parker, P. L.: Recycling of elements transported upstream by runs of Pacific salmon: 1, $\delta^{15}\text{N}$ and $\delta^{13}\text{C}$ evidence in Sashin Creek, southeastern Alaska, *Can. J. Fish. Aquat. Sci.*, 47, 136-144, <https://doi.org/10.1139/F90-014>, 1990.
- Koyama, A., Kavanagh, K., and Robinson, A.: Marine nitrogen in central Idaho riparian forests: evidence from stable isotopes, *Can. J. Fish. Aquat. Sci.*, 62, 518-526, <https://doi.org/10.1139/F04-220>, 2005.
- 460 Liang, C., Schimel, J. P., and Jastrow, J. D.: The importance of anabolism in microbial control over soil carbon storage, *Nat. Microbiol.*, 2, <https://doi.org/10.1038/Nmicrobiol.2017.105>, 2017.
- Lodge, D. J., Winter, D., Gonzalez, G., and Clum, N.: Effects of hurricane-felled tree trunks on soil carbon, nitrogen, microbial biomass, and root length in a wet tropical forest, *Forests*, 7, <https://doi.org/10.3390/F7110264>, 2016.
- 465 Macdonald, B. C. T., Farrell, M., Tuomi, S., Barton, P. S., Cunningham, S. A., and Manning, A. D.: Carrion decomposition causes large and lasting effects on soil amino acid and peptide flux, *Soil Biol. Biochem.*, 69, 132-140, <https://doi.org/10.1016/j.soilbio.2013.10.042>, 2014.
- 470 Martinelli, L. A., Piccolo, M. C., Townsend, A. R., Vitousek, P. M., Cuevas, E., McDowell, W., Robertson, G. P., Santos, O. C., and Treseder, K.: Nitrogen stable isotopic composition of



- leaves and soil: tropical versus temperate forests, *Biogeochemistry*, 46, 45-65,
<https://doi.org/10.1023/A:1006100128782>, 1999.
- 475 McClain, M. E., Boyer, E. W., Dent, C. L., Gergel, S. E., Grimm, N. B., Groffman, P. M., Hart,
S. C., Harvey, J. W., Johnston, C. A., Mayorga, E., McDowell, W. H., and Pinay, G.:
Biogeochemical hot spots and hot moments at the interface of terrestrial and aquatic
ecosystems, *Ecosystems*, 6, 301-312, <https://doi.org/10.1007/s10021-003-0161-9>, 2003.
- Melis, C., Selva, N., Teurlings, I., Skarpe, C., Linnell, J. D. C., and Andersen, R.: Soil and
480 vegetation nutrient response to bison carcasses in Bialeowieza Primeval Forest, Poland, *Ecol.
Res.*, 22, 807-813, <https://doi.org/10.1007/s11284-006-0321-4>, 2007.
- Metcalfe, J. L., Parfrey, L. W., Gonzalez, A., Lauber, C. L., Knights, D., Ackermann, G.,
Humphrey, G. C., Gebert, M. J., Van Treuren, W., Berg-Lyons, D., Keepers, K., Guo, Y.,
Bullard, J., Fierer, N., Carter, D. O., and Knight, R.: A microbial clock provides an accurate
485 estimate of the postmortem interval in a mouse model system, *Elife*, 2,
<https://doi.org/10.7554/eLife.01104>, 2013.
- Natelhofer, K. J., and Fry, B.: Controls on natural ^{15}N and ^{13}C abundances in forest soil organic
matter, *Soil Sci. Soc. Am. J.*, 52, 1633-1640, 1988.
- Parmenter, R. R., and Lamarra, V. A.: Nutrient cycling in a freshwater marsh: the decomposition
490 of fish and waterfowl carrion, *Limnol. Oceanogr.*, 36, 976-987, 1991.
- Parmenter, R. R., and MacMahon, J. A.: Carrion decomposition and nutrient cycling in a
semiarid shrub-steppe ecosystem, *Ecol. Monogr.*, 79, 637-661, <https://doi.org/10.1890/08-0972.1>, 2009.



- Parnell, A. C., Inger, R., Bearhop, S., and Jackson, A. L.: Source partitioning using stable
495 isotopes: coping with too much variation, PLoS One, 5,
<https://doi.org/10.1371/journal.pone.0009672>, 2010.
- Payne, J. A.: A summer carrion study of the baby pig *Sus scrofa* Linnaeus, Ecology, 46, 592-
602, <https://doi.org/10.2307/1934999>, 1965.
- Putman, R. J.: Dynamics of the blowfly, *Calliphora erythrocephala*, within carrion, J. Anim.
500 Ecol., 46, 853-866, 1977.
- R core team, R: A language and environment for statistical computing: [https://www.R-
project.org/](https://www.R-project.org/), version 3.5.0, 2018.
- Redmile-Gordon, M. A., Armenise, E., White, R. P., Hirsch, P. R., and Goulding, K. W. T.: A
comparison of two colorimetric assays, based upon Lowry and Bradford techniques, to
505 estimate total protein in soil extracts, Soil Biol. Biochem., 67, 166-173,
<https://doi.org/10.1016/j.soilbio.2013.08.017>, 2013.
- Rhine, E. D., Sims, G. K., Mulvaney, R. L., and Pratt, E. J.: Improving the Berthelot reaction for
determining ammonium in soil extracts and water, Soil Sci. Soc. Am. J., 62, 473-480, 1998.
- Robinson, D.: $\delta^{15}\text{N}$ as an integrator of the nitrogen cycle, Trends Ecol. Evol., 16, 153-162,
510 [https://doi.org/10.1016/S0169-5347\(00\)02098-X](https://doi.org/10.1016/S0169-5347(00)02098-X), 2001.
- Soil Survey Staff, Web Soil Survey, Natural Resources Conservation Service, United States
Department of Agriculture: <https://websoilsurvey.sc.egov.usda.gov/>, Accessed 29 May 2018.
- Szelecz, I., Koenig, I., Seppey, C. V. W., Le Bayon, R. C., and Mitchell, E. A. D.: Soil chemistry
changes beneath decomposing cadavers over a one-year period, Forensic Sci. Int., 286, 155-
515 165, <https://doi.org/10.1016/j.forsciint.2018.02.031>, 2018.



- Towne, E. G.: Prairie vegetation and soil nutrient responses to ungulate carcasses, *Oecologia*, 122, 232-239, <https://doi.org/10.1007/P100008851>, 2000.
- van der Waal, C., Kool, A., Meijer, S. S., Kohi, E., Heitkonig, I. M. A., de Boer, W. F., van Langevelde, F., Grant, R. C., Peel, M. J. S., Slotow, R., de Knecht, H. J., Prins, H. H. T., and
520 de Kroon, H.: Large herbivores may alter vegetation structure of semi-arid savannas through soil nutrient mediation, *Oecologia*, 165, 1095-1107, <https://doi.org/10.1007/s00442-010-1899-3>, 2011.
- Vidon, P., Allan, C., Burns, D., Duval, T. P., Gurwick, N., Inamdar, S., Lowrance, R., Okay, J., Scott, D., and Sebestyen, S.: Hot spots and hot moments in riparian zones: potential for
525 improved water quality management, *J. Am. Water Resour. Assoc.*, 46, 278-298, <https://doi.org/10.1111/j.1752-1688.2010.00420.x>, 2010.
- Wheeler, T. A., Kavanagh, K. L., and Daanen, S. A.: Terrestrial salmon carcass decomposition: nutrient and isotopic dynamics in central Idaho, *Northwest Sci.*, 88, 106-119, <https://doi.org/10.3955/046.088.0206>, 2014.
- 530 Wheeler, T. A., and Kavanagh, K. L.: Soil biogeochemical responses to the deposition of anadromous fish carcasses in inland riparian forests of the Pacific Northwest, USA, *Can. J. Forest Res.*, 47, 1506-1516, <https://doi.org/10.1139/cjfr-2017-0194>, 2017.
- Wright, S. F., and Upadhyaya, A.: Extraction of an abundant and unusual protein from soil and comparison with hyphal protein of arbuscular mycorrhizal fungi, *Soil Sci.*, 161, 575-586,
535 <https://doi.org/10.1097/00010694-199609000-00003>, 1996.



Table 1: Selected soil biogeochemical data during one year of decomposition. Letters indicate significant differences between samples based on One-way ANOVA ($p < 0.05$). Asterisks indicate significant differences between control and treatment soils.

	Sampling Date	Soil Gravimetric Moisture	pH	Conductivity ($\mu\text{S cm}^{-1}$)	Dissolved Oxygen (%)	Total carbon (%)	Total nitrogen (%)	C/N	$\delta^{15}\text{N}$	$\delta^{13}\text{C}$
<i>Initial</i>	29 July	0.299 ± 0.012 ^{AB}	6.79 ± 0.1 ^A	47.83 ± 5.9 ^{AC}	98.5 ± 0.29 ^A	5.11 ± 0.101	0.295 ± 0.009	17.33 ± 0.25 ^{AC}	1.48 ± 0.23 ^A	-27.86 ± 0.08
<i>Early</i>	1 August	0.216 ± 0.034 ^A	6.86 ± 0.3 ^A	73.53 ± 32.2 ^A	N.M.	3.927 ± 1.08	0.245 ± 0.058	15.93 ± 1.7 ^{AC}	2.65 ± 1.66 ^A	-27.73 ± 0.42
Early control	1 August	0.219	6.82	36.78	N.M.	4.196	0.247	16.99	1.76	-27.56
<i>Active</i>	3 August	0.234 ± 0.056 ^A	8.64 ± 0.3 ^B	2150.48 ± 1282 ^{BC}	9.16 ± 7.89 ^{BC}	4.251 ± 0.798	0.362 ± 0.096	12.01 ± 1.34 ^{BC}	6.23 ± 1.50 ^B	-27.77 ± 0.30
Active control	3 August	0.160	6.68*	31.65*	98.6 ± 1.25*	4.159	0.267	15.58*	1.48*	-27.68
<i>Advanced</i>	9 August	0.286 ± 0.081 ^{AB}	8.78 ± 0.1 ^B	1233 ± 494 ^C	19.4 ± 31.2 ^B	4.000 ± 1.29	0.303 ± 0.080	13.07 ± 0.75 ^{BC}	8.72 ± 2.09 ^B	-27.64 ± 0.20
Advanced control	9 August	0.223	6.84*	43.42*	98.0 ± 0.57*	5.008	0.281	17.82*	1.26*	-27.77
<i>Early skeletal</i>	6 September	0.242 ± 0.070 ^A	7.58 ± 0.4 ^C	973.8 ± 211 ^{AC}	97.4 ± 0.84 ^{AC}	3.610 ± 0.839	0.293 ± 0.057	12.28 ± 0.74 ^{BC}	9.26 ± 1.54 ^B	-27.74 ± 0.30
Early skeletal control	6 September	0.121	6.84*	35.08	98.3 ± 0.50	4.023	0.259	15.53*	1.78*	-27.63
<i>Late skeletal</i>	9 December	0.271 ± 0.021 ^{AB}	6.93 ± 0.3 ^A	225.2 ± 84.8 ^{AC}	100 ± 0 ^A	2.668 ± 0.352	0.214 ± 0.030	12.51 ± 0.67 ^{BC}	9.25 ± 1.33 ^B	-27.41 ± 0.25
Late skeletal control	9 December	0.246	6.73	29.13	100 ± 0	2.084	0.136	15.37*	1.79*	-27.30
<i>1 yr. post decay</i>	10 August	0.404 ± 0.027 ^B	6.10 ± 0.3 ^D	29.47 ± 7.6 ^A	N.M.	4.253 ± 1.07	0.285 ± 0.036	15.24 ± 3.49 ^C	8.42 ± 1.52 ^B	-27.67 ± 0.25
1 yr. post decay control	10 August	0.449*	6.29*	23.07	N.M.	4.36	0.26	17.08	0.05*	-27.73



540 Table 1 (continued):

	Protein (mg g ⁻¹)	Microbial respiration rate (µg CO ₂ -C release gdw ⁻¹ day ⁻¹)	DOC (µg C gdw ⁻¹)	Ammonium (mg NH ₄ -N gdw ⁻¹)	Nitrification potential rate (mg NO ₂ gdw ⁻¹ day ⁻¹)	Nitrate (mg NO ₃ ⁻ -N gdw ⁻¹)	DON (mg N gdw ⁻¹)	Accumulated Degree Days (ADD)
<i>Initial</i>	0.251 ± 0.051	50.9 ± 8 ^A	2.44 ± 0.2 ^{AC}	0.039 ± 0.01 ^A	0.181 ± 0.05 ^A	0.000 ± 0.0 ^A	0.283 ± 0.02 ^A	26.1
<i>Early</i>	0.200 ± 0.037	51.4 ± 18 ^A	3.44 ± 1.0 ^A	0.101 ± 0.06 ^A	0.237 ± 0.16 ^A	0.000 ± 0.0 ^A	0.718 ± 0.35 ^A	106.7
Early control	0.159 ± 0.004	35.2	2.35	0.011	0.167	0.000	0.242	106.7
<i>Active</i>	0.260 ± 0.025	300 ± 90 ^B	66.54 ± 40.4 ^B	2.49 ± 1.24 ^B	0.366 ± 0.09 ^A	0.001 ± 0.0 ^A	1.363 ± 1.4 ^A	160.3
Active control	0.225 ± 0.007	27.8*	2.52*	0.010*	0.163	0.000	0.205	160.3
<i>Advanced</i>	0.281 ± 0.072	162.8 ± 110 ^A	42.5 ± 30.0 ^C	2.29 ± 1.80 ^{BC}	0.517 ± 0.17 ^A	0.001 ± 0.0 ^A	1.906 ± 1.7 ^A	321.7
Advanced control	0.239 ± 0.024*	45.7*	3.44*	0.015*	0.181	0.003	0.304	321.7
<i>Early skeletal</i>	0.238 ± 0.049	76.9 ± 42 ^A	14.3 ± 3.4 ^{AC}	0.775 ± 0.14 ^{AC}	8.57 ± 4.4 ^B	0.309 ± 0.169 ^B	6.089 ± 1.24 ^B	1042.8
Early skeletal control	0.193 ± 0.021	20.8	2.89	0.006	0.130*	0.000*	0.185*	1042.8
<i>Late skeletal</i>	0.250 ± 0.014	57.2 ± 26 ^A	10.2 ± 8.4 ^{AC}	0.246 ± 0.06 ^A	0.017 ± 0.20 ^A	0.019 ± 0.001 ^A	1.929 ± 0.37 ^A	2591.7
<i>Late skeletal control</i>	0.195 ± 0.016	46.5	3.12	0.012	0.039	0.000	0.309	2591.7
<i>1 yr. post decay</i>	0.239 ± 0.021	64.1 ± 8^A	2.81 ± 0.5^A	0.008 ± 0.0^A	0.006 ± 0.00^A	0.001 ± 0.0^A	0.095 ± 0.01^A	6377.5
<i>1 yr. post decay control</i>	0.195 ± 0.008	59.5	2.43 ± 0.0	0.007	0.006	0.000	0.093	6377.5



Table 2: Differences in soil $\delta^{15}\text{N}$ at depth and $\delta^{15}\text{N}$ in surface soils for hotspot and control depth profiles.

Depth (cm)	$\Delta^{15}\text{N}$ (‰)	
	Hotspot	Control
0	0	0
5	-2.1	2.65
10	-1.5	3.2
15	0.1	6.6
20	0.9	7.7
30	0.9	6.1
40	1.2	8.4

545



Figure 1

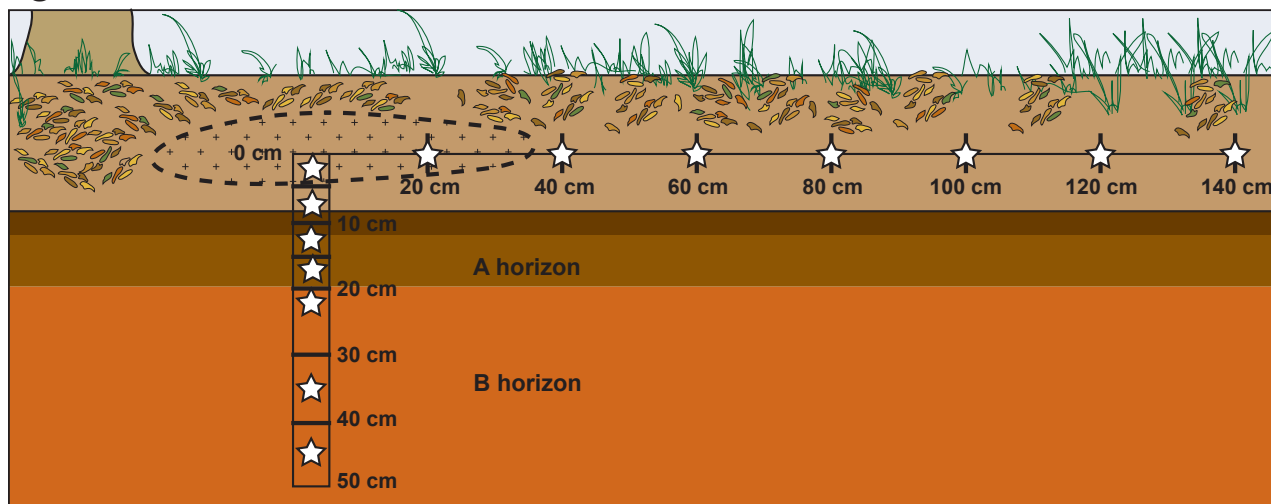




Figure 2





Figure 3

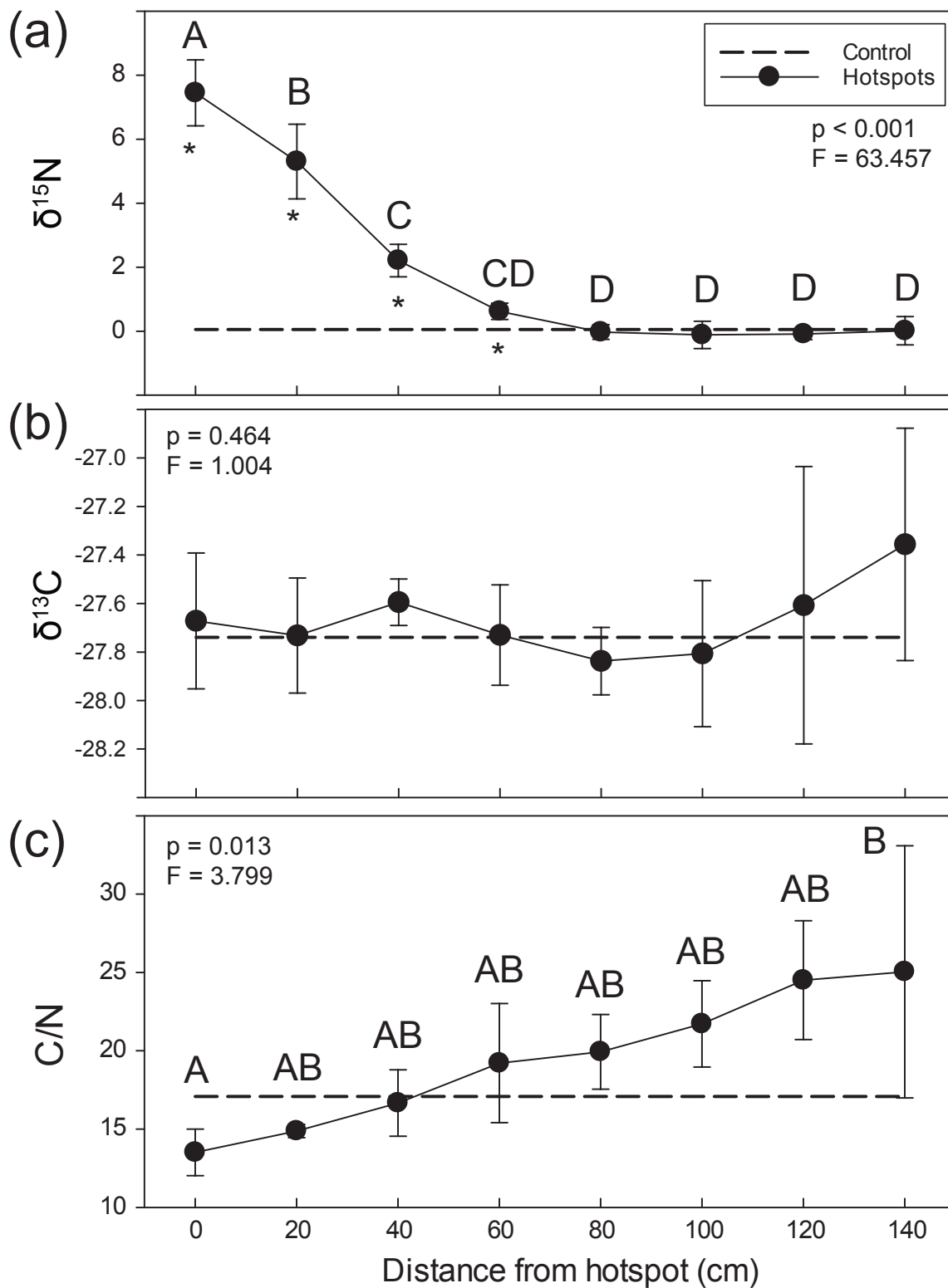




Figure 4

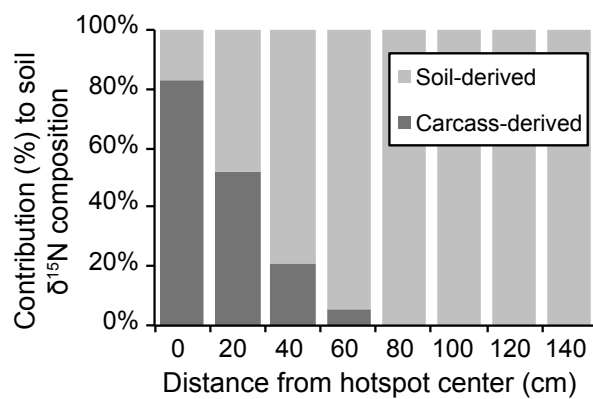




Figure 5

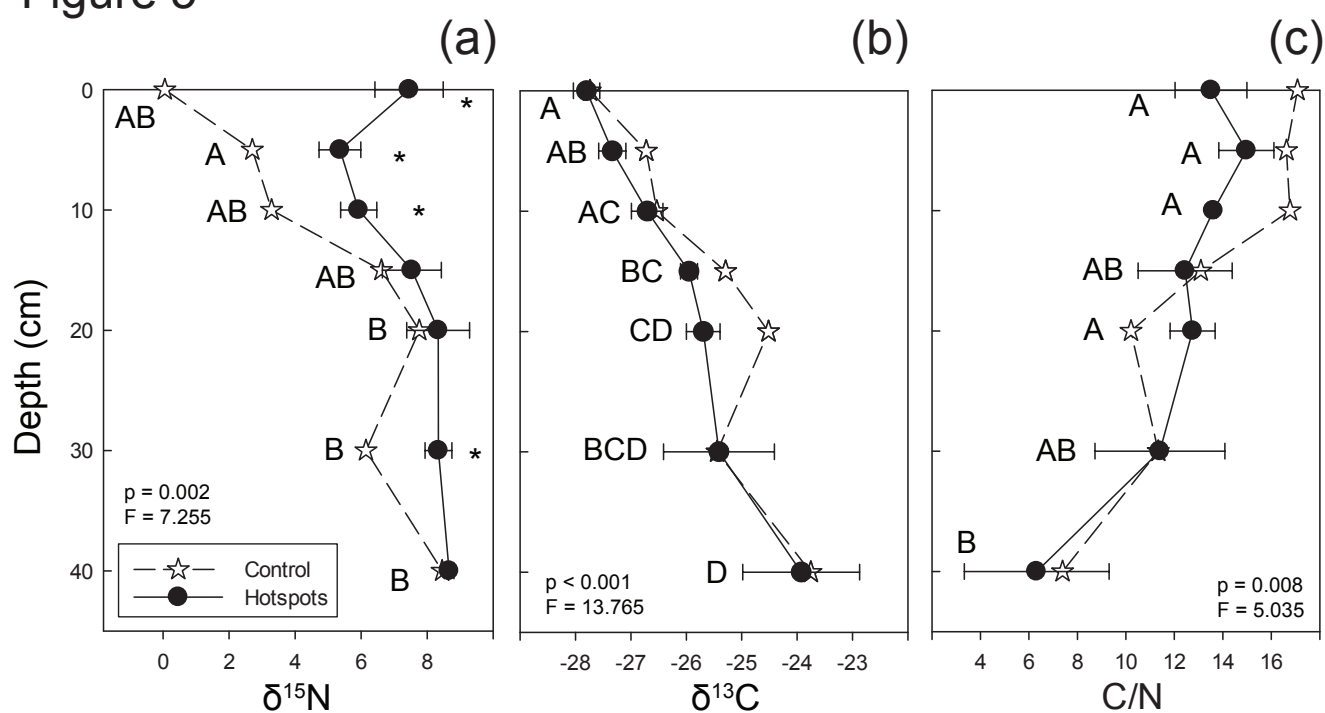




Figure 6

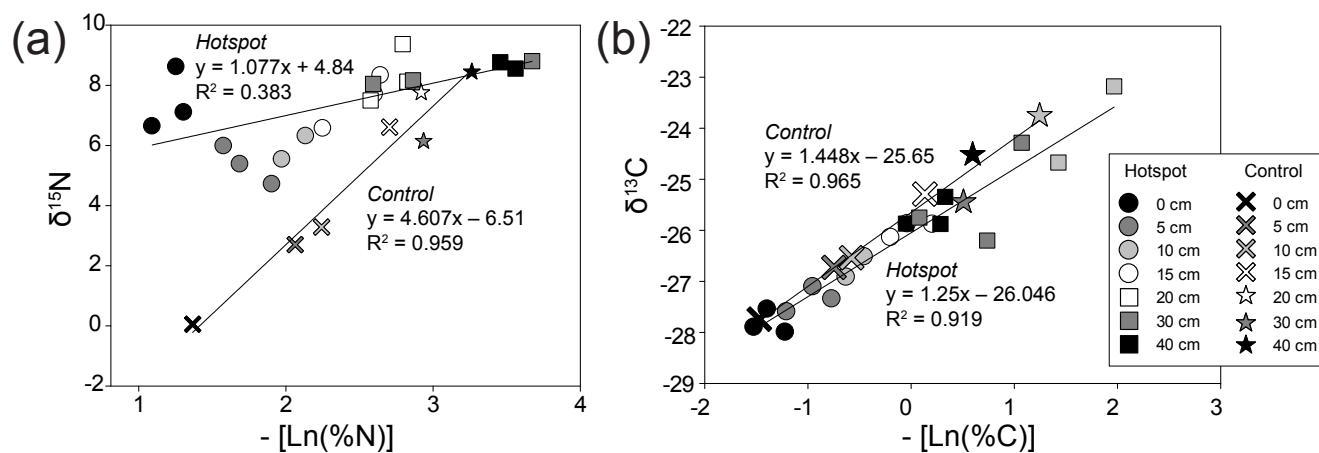




Figure 7

